Mon. Not. R. Astron. Soc. **000**, 1–11 (2009) Printed 23 December 2009 (MN LATEX style file v2.2)

Pulsations in the atmosphere of the roAp star HD 24712 II. Theoretical models

Hideyuki Saio[(1)⋆], Tanya Ryabchikova[(2)], and Mikhail Sachkov[(2)]
[(1)] *Astronomical Institute, Graduate School of Science, Tohoku University, Sendai, 980-8578, Japan*
[(2)] *Institute of Astronomy, Russian Academy of Science, Pyatnitskaya 48, 119017 Moscow, Russia*

ABSTRACT

We discuss pulsations of the rapidly oscillating Ap (roAp) star HD 24712 (HR 1217) based on nonadiabatic analyses taking into account the effect of dipole magnetic fields. We have found that all the pulsation modes appropriate for HD 24712 are damped; i.e., the kappa-mechanism excitation in the hydrogen ionization layers is not strong enough to excite high-order p-modes with periods consistent with observed ones, all of which are found to be above the acoustic cut-off frequencies of our models.

The main (2.721 mHz) and the highest (2.806 mHz) frequencies are matched with modified $l = 2$ and $l = 3$ modes, respectively. The large frequency separation ($\approx$ 68 μHz) is reproduced by models which lay within the error box of HD 24712 on the HR diagram. The nearly equally spaced frequencies of HD 24712 indicate the small frequency separation to be as small as $\approx$ 0.5 μHz. However, the small separation derived from theoretical $l = 1$ and 2 modes are found to be larger than ~ 3 μHz. The problem of equal spacings could be resolved by assuming that the spacings correspond to pairs of $l = 2$ and $l = 0$ modes; this is possible because magnetic fields significantly modify the frequencies of $l = 0$ modes. The amplitude distribution on the stellar surface is strongly affected by the magnetic field resulting in the predominant concentration at the polar regions. The modified amplitude distribution of a quasi-quadrapole mode predicts a rotational amplitude modulation consistent with the observed one.

Amplitudes and phases of radial-velocity variations for various spectral lines are converted to relations of amplitude/phase versus optical depth in the atmosphere. Oscillation phase delays gradually outward in the outermost layers indicating the presence of waves propagating outward. The phase changes steeply around $\log \tau \sim -3.5$, which supports a $T - \tau$ relation having a small temperature inversion there.

Key words: stars:individual:HD 24712 – stars:magnetic fields – stars: oscillations

1 INTRODUCTION

HD 24712 (HR 1217, DO Eri) is a prototype of the rapidly oscillating Ap (roAp) stars that consist of about 40 members. The oscillations, with periods ranging from ~ 6 to ~ 20 min, are high radial-order p-modes affected by strong magnetic fields of 1 kG to 25 kG.

The 6.15 minute light variation of HD 24712 was discovered by Kurtz (1981). Matthews et al. (1988) first discovered radial velocity (RV) variations with an amplitude of $400 \pm 50\,\mathrm{m\,s^{-1}}$. A WET (Whole Earth Telescope) campaign found eight frequencies with rotational side-lobes as presented in Kurtz et al. (2005); the paper also gives a thorough review of preceding research on this star. From accurate RV measurements Mkrtichian & Hatzes (2005) obtained two additional frequencies. Ryabchikova et al. (2007) (Paper I) studied oscillation amplitudes and phases corresponding to the two highest amplitude modes for ≈600 unblended spectral lines of different elements/ions, and found a diversity of these pulsational characteristics in two thirds of them.

The magnetic field of HD 24712 has been studied by many authors as reviewed in Ryabchikova et al. (1997). Bagnulo et al. (1995) derived a polar magnetic strength of $B_p = 3.9$ kG, a rotational inclination (angle between line-of-sight and rotation axis) of $i = 137^\circ$ (or 43°) and a magnetic obliquity (the angle between the rotation and magnetic axes) of $\beta = 150^\circ$ (or 30°). Ryabchikova et al. (1997) found that a slightly higher strength of $B_p = 4.4$ kG is more consistent with their polarimetric observations. Recently, by inverting rotationally modulated polarized spectra, Lüftinger et al. (2008) found that HD 24712 has a nearly dipole magnetic

⋆ saio@astr.tohoku.ac.jp

field with the strength varying between 2.2 kG and 4.4 kG, depending on the rotation phase.

One of the reasons why oscillations of roAp stars are important lies in the fact that many (often regularly spaced) oscillation frequencies are excited simultaneously giving great potential for asteroseismic studies. One difficulty in applying asteroseismology to roAp stars is that strong magnetic fields affect the high-order p-modes in complex ways. Although the frequency of an oscillation mode generally increases with increasing magnetic field strength, it occasionally jumps down by ~ 10 to $30\,\mu$Hz and then starts increasing again (Cunha & Gough 2000; Saio & Gautschy 2004). At present, there are three independent methods to calculate magnetic effects on high-order p-modes: the method of Cunha & Gough (2000) is based on a variational principle, the other two use truncated expansions with spherical harmonics to present the angular dependences of eigenfunctions (Dziembowski & Goode 1996; Bigot et al. 2000; Saio & Gautschy 2004). The results from those three methods roughly agree with each other as discussed by Cunha (2006) and by Saio (2008).

A further complexity arises if the rotation effect is taken into account. Bigot & Dziembowski (2002) investigated the oscillation properties taking into account both effects of rotation and magnetic field. In our present investigation, however, we disregard the effect of rotation on the frequency and eigenfunctions for simplicity, hoping that the effect is small because the pulsation periods, ~ 6 min, are very much shorter than the ≈ 12-d rotation period of HD 24712.

Previously, theoretical pulsation models based on the method of Saio (2005) were compared with the observed frequencies for γ Equ (Gruberbauer et al. 2008), 10 Aql (Huber et al. 2008) and HD 101065 (Mkrtichian et al. 2008). Those attempts were more-or-less successful, although the required strength of the magnetic fields in models tended to be larger than that measured by the Zeeman splittings of spectral lines. In this paper we provide the same modelling of HD 24712 and for the first time we compare not only oscillation frequencies but also the amplitude and phase variations in the atmosphere of HD 24712.

2 MODELS

2.1 Unperturbed models

For unperturbed models, we adopted spherically symmetric evolutionary models calculated with OPAL opacity tables (Iglesias & Rogers 1996). Table 1 lists various assumptions adopted for each series of evolutionary models. Except for AH165C, envelope convection is suppressed, assuming a strong magnetic field to stabilize convection. For the envelope convection included in AH165C we used a local mixing-length theory with a mixing-length of 1.5 times the pressure scale height.

We considered two types of $T-\tau$ relations in the optically thin outer layers (Fig. 1). One of them is a standard relation (denoted as "SS" in Table 1) obtained from eq. (10) of Shibahashi & Saio (1985). The other one (denoted as "Ap" in Table 1) is a relation obtained by Shulyak et al. (2009) for the self-consistent atmospheric model of HD 24712 that takes into account element stratification including rare-earth elements. The latter relation has a small temperature inversion at $\log \tau_{5000} \approx -3.5$ where abundances of praseodymium (Pr) and neodymium (Nd) increase steeply outward. (Although the optical depth in Shulyak et al.'s relation refers to τ_{5000}, optical depth at a wavelength of 5000 Å, we assume in our present paper that τ_{5000} is not very different from Rosseland-mean optical depth τ.)

We have computed models with and without helium depletion in the outermost layers (the 6th column of Table 1). In the helium depleted models, the helium abundance is calculated as $Y = 0.01 + (Y_i - 0.01) \times (x_2 + x_3)$ (cf. Balmforth et al. 2001), where Y_i is the (initial) helium abundance in the interior, x_2 and x_3 are fractions of He II and He III, respectively.

Fig. 2 shows the evolutionary tracks of AD160, AD165, AD170, AD170Z25, and AD150Z1 with the position of HD 24712 with error bars. The type of $T-\tau$ relation, on/off

Table 1. Unperturbed model parameters

Name	$M/M_\odot$	X	Z	$T(\tau)$	He-dep.	conv
AD160	1.60	0.70	0.02	Ap	Y	N
AD165	1.65	0.70	0.02	Ap	Y	N
AD170	1.70	0.70	0.02	Ap	Y	N
AH165	1.65	0.70	0.02	Ap	N	N
AH165C	1.65	0.70	0.02	Ap	N	Y
AD170Z25	1.70	0.695	0.025	Ap	Y	N
AH170Z25	1.70	0.695	0.025	Ap	N	N
AD150Z1	1.50	0.71	0.01	Ap	Y	N
AH150Z1	1.50	0.71	0.01	Ap	N	N
SD160	1.60	0.70	0.02	SS	Y	N
SD165	1.65	0.70	0.02	SS	Y	N
SD170	1.70	0.70	0.02	SS	Y	N
SH165	1.65	0.70	0.02	SS	N	N

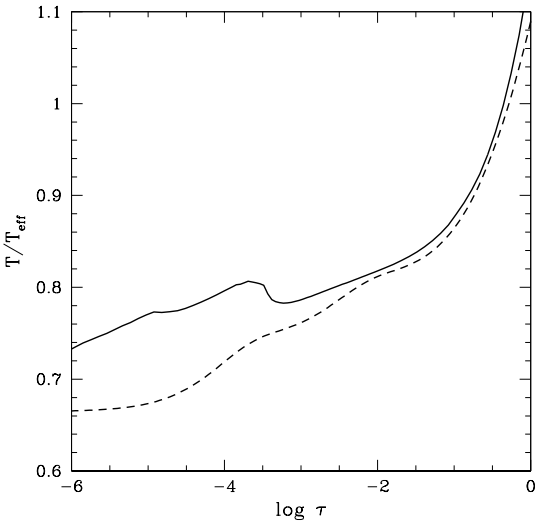

Figure 1. Two types of $T-\tau$ relations employed. The standard relation (dashed line) is obtained from eq. (10) of Shibahashi & Saio (1985), while the Ap star relation (solid line) is adopted from Shulyak et al. (2009).

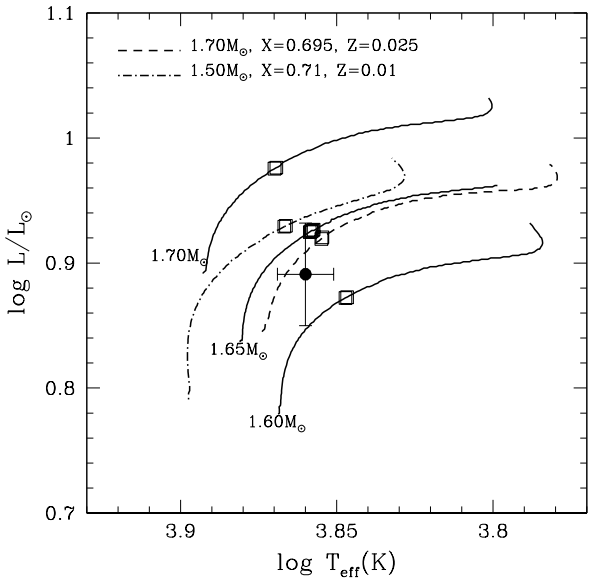

Figure 2. Evolutionary tracks and the position of HD 24712 with error bars. Solid lines show the evolutionary tracks for a standard composition of $(X, Z) = (0.7, 0.02)$. Open squares indicate the loci of models giving best fits to the observed frequencies for various cases listed in Table 1. At those positions, models have large frequency separations similar to 68 μHz, which is determined mainly by stellar mass and radius.

of the He-depletion, and on/off of the envelope convection hardly change the evolutionary tracks on the HR diagram. The stellar masses for the metal rich ($Z = 0.025$) and metal poor ($Z = 0.01$) cases are chosen such that the evolutionary tracks pass close to the position of HD 24712.

We have adopted the effective temperature $T_{\rm eff} = 7250 \pm 150\,{\rm K}$ (or $\log T_{\rm eff} = 3.860 \pm 0.009$) obtained by Ryabchikova et al. (1997) and confirmed by Shulyak et al. (2009). The range of effective temperature is consistent with $T_{\rm eff} = 7330 \pm 140\,{\rm K}$ derived by Wade (1997) and $T_{\rm eff} = 7350\,{\rm K}$ determined by Lüftinger et al. (2008).

Shulyak et al. (2009) estimated the radius of HD 24712 to be $R = 1.772 \pm 0.043 {\rm R}_\odot$ by combining the spectral energy distribution and the Hipparcos parallax $\pi = 20.32 \pm 0.39$ mas (van Leeuwen 2007). These estimates for the effective temperature and radius yield $\log L/{\rm L}_\odot = 0.891 \pm 0.041$ for the luminosity of HD 24712, which was used to place HD 24712 on the HR diagram (Fig. 2). We note that the adopted luminosity and temperature of HD 24712 are consistent with the values used in previous analysis by Cunha et al. (2003) ($\log L/{\rm L}_\odot = 0.892 \pm 0.041$ and $\log T_{\rm eff} = 3.869^{+0.006}_{-0.012}$), where the luminosity (based on the Hipparcos parallax) was taken from Matthews et al. (1999).

2.2 Pulsation Models

We have obtained nonadiabatic frequencies and eigenfunctions for axisymmetric high-order p-modes based on the method described in Saio (2005) except for the outer-boundary condition and the perturbation of radiation. Since all of the observed oscillation frequencies in HD 24712 are above the acoustic cut-off frequencies of the models considered here, we used a running wave condition for the mechanical outer boundary condition at $\log \tau \approx -6$.

Applying a standard method (see e.g., Unno et al. 1989) to the mechanical equations (A3) and (A4) of Saio (2005), we obtain a running-wave condition as

$$\frac{V}{2\chi_\rho}\left[1 - i\sqrt{4\omega^2\chi_\rho/V - 1}\right]\boldsymbol{Y}_2 = \omega^2 \boldsymbol{Y}_1, \quad (1)$$

where $\chi_\rho \equiv (\partial \ln P/\partial \ln \rho)_T$ with P and ρ being pressure and matter density, respectively, and the other symbols are the same as in Saio (2005). In deriving the equation we have assumed the oscillations are isothermal at the outer boundary.

In calculating the perturbation of radiation flux, we have adopted the Unno & Spiegel (1966) theory for the Eddington approximation, where the radiative flux is given as

$$\boldsymbol{F}_{\rm rad} = -\frac{1}{3\kappa\rho}\nabla\left(acT^4 + \frac{1}{\kappa}\frac{dS}{dt}\right), \quad (2)$$

where S, κ, a, and c are entropy per unit mass, opacity per unit mass, the radiation constant, and the speed of light, respectively. We used a linearized form of the above equation (Saio & Cox 1980). Including the dS/dt term with the running wave boundary condition is found to reduce the oscillation phase variation in the outermost layers making it consistent with observations.

The angular dependences of eigenfunctions are expanded using axisymmetric spherical harmonics $Y_\ell^{m=0}$ (i.e., Legendre polynomials) with $\ell = 2j - 2$ (even modes) or $\ell = 2j - 1$ (odd modes), where $j = 1, 2, \ldots j_t$. An even (odd) mode is symmetric (anti-symmetric) with respect to the magnetic equator. The expansion is truncated as $j_t = 12$ in most cases; but sometimes $j_t = 14$ is adopted to have better accuracy in frequencies. To label the type of angular dependence of a mode we use l_m which is equal to the ℓ value of the component having the maximum kinetic energy among the expansion components. We note that the angular distribution of amplitude varies depending on the strength of magnetic field even for a fixed l_m. To represent the strength of a dipole magnetic field we use the polar strength B_p.

3 THEORETICAL RESULTS AND COMPARISONS TO OBSERVATIONS

3.1 Oscillation frequencies

We calculated nonadiabatic oscillation frequencies between ~ 2.5 mHz and ~ 2.9 mHz for $0 \leqslant l_m \leqslant 3$ including the effect of dipole magnetic fields in a range of $2 \leqslant B_p/({\rm kG}) \leqslant 7$. For the series listed in Table 1, we performed pulsation analyses for models having large frequency spacings comparable with that of HD 24712; i.e., 68 μHz.

All the pulsation modes having frequencies comparable with the observed ones are found to be damped; i.e., no excited modes are found. The excitation mechanism for the oscillations of roAp stars is generally thought to be the κ-mechanism in the hydrogen ionization zone (Balmforth et al. 2001; Cunha 2002). For cool roAp stars like HD 24712 and HD 101065 (Mkrtichian et al. 2008), however, the κ-mechanism seems not strong enough. The

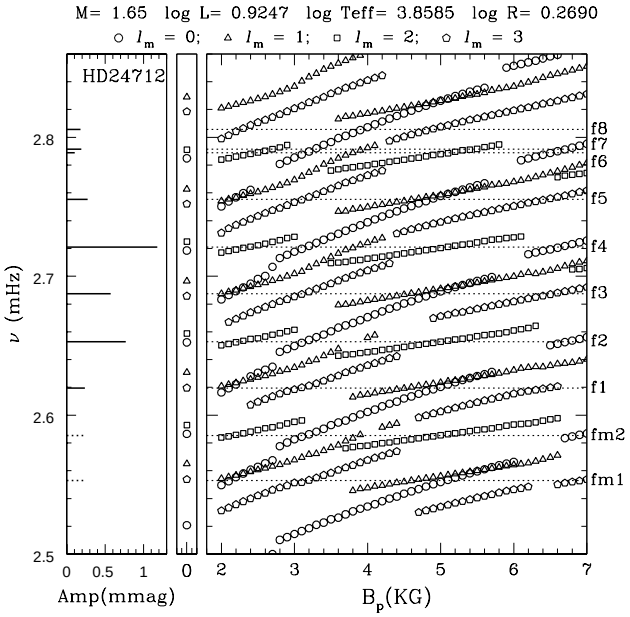

Figure 3. Observed oscillation frequencies and amplitudes of HD 24712 (left panel) and theoretical frequencies as a function of B_p (the strength of magnetic field at poles) for a model in the series AD165 (right panel). In the left panel, solid lines show frequencies and the photometric amplitudes obtained by the WET campaign (f1–f8; Kurtz et al. 2005), while dotted lines represent additional two frequencies (fm1 and fm2) obtained by the radial velocity observation by Mkrtichian & Hatzes (2005), the amplitudes of which are set arbitrary equal to the amplitude of the WET lowest frequency. The label for each frequency is indicated along the rightmost vertical axis. The middle panel shows theoretical frequencies obtained without including the magnetic effects. Horizontal dotted lines in the right panel indicate the observed frequencies.

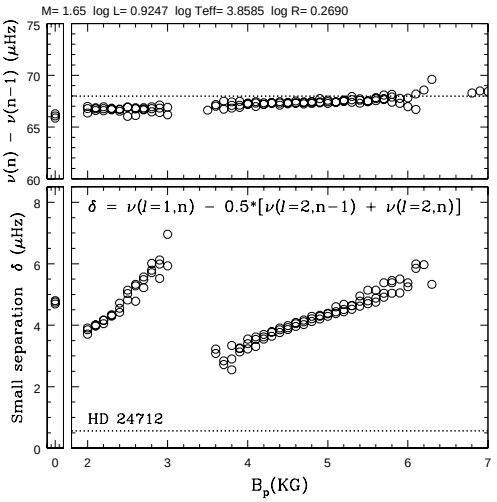

Figure 4. Large separation (top panel) and small separation (bottom panel) of frequencies as functions of B_p for the model shown in Fig. 3. Dotted lines indicate observed large and small separations of HD 24712.

temperature inversion (Fig. 1) is too small to help excite high-order p-modes as discussed in Gautschy et al. (1998). It seems that we need a new excitation mechanism for cool roAp stars.

Fig. 3 shows an example of p-mode frequencies in a model as a function of B_p (the magnetic-field strength at poles). The observed frequencies by a WET campaign (Kurtz et al. 2005) and the radial velocity observation by Mkrtichian et al. (2008) are also shown. Different symbols correspond to different values of l_m. Generally, the frequency of an oscillation mode increases with B_p, but occasionally it jumps down by ~ 30 μHz and then starts increasing again. This property was discovered by Cunha & Gough (2000) and confirmed by Saio & Gautschy (2004). The expansion method adopted in this investigation fails around the frequency jump, where the distribution of kinetic energy among the components of expansion is broad.

Frequencies of different radial order for a given l_m vary approximately parallel as a function of B_p so that the large frequency separation $\Delta\nu$ hardly changes with B_p, where $\Delta\nu \equiv \nu(l_m; n) - \nu(l_m; n-1)$ with n being the radial order of a mode. The top panel of Fig. 4 shows $\Delta\nu$ calculated for $l_m = 2$ modes in the model shown in Fig. 3. The large separation increases very slowly as a function of B_p. This corresponds to an increase in the phase velocity of magneto-acoustic wave, $\sqrt{c_s^2 + v_A^2}$, with B_p, where c_s and v_A are the adiabatic sound speed and the Alfvén speed, respectively.

The bottom panel of Fig. 4 shows the small separation defined as

$$\delta = \nu(l_m = 1; n) - 0.5[\nu(l_m = 2; n-1) + \nu(l_m = 2; n)] \quad (3)$$

calculated using the frequencies shown in Fig. 3. The small separation of the model is about $5\,\mu$Hz at $B_p = 0$. In the presence of a magnetic field, δ varies from $\sim 3\,\mu$Hz to $\sim 6\,\mu$Hz. Generally, δ increases with B_p, but it jumps down at the frequency jumps discussed above. The gradual growth of δ comes from the fact that the frequencies of $l_m = 1$ modes increase slightly more steeply with B_p than those of $l_m = 2$ modes. Just after the jump, δ reaches a minimum which is considerably smaller than in the case of $B_p = 0$, but still significantly larger than the observed value $\sim 0.5\,\mu$Hz, obtained by assuming that f3 is a $l_m = 1$ mode and f2 and f4 are $l_m = 2$ modes. Such a small value of δ cannot be reproduced by any model examined in the present paper. The problem of the small spacing of HD 24712 is not unique. Bruntt et al. (2009) found a small spacing that is essentially zero in another roAp star α Cir – very much smaller than that of HD 24712. It is important to solve this problem of the small spacing; it could be related to a fundamental property of roAp stars.

A relatively large theoretical δ means that the frequency of an $l_m = 1$ mode is slightly larger than the mean of the adjacent two $l_m = 2$ modes. It is interesting to note that $l_m = 0$ modes cross $l_m = 1$ modes at $B_p \approx 5$ kG (Fig. 3). In other words, the frequency of each $l_m = 0$ mode is slightly smaller than the frequency of the adjacent $l_m = 1$ mode at $B_p \approx 5$ kG. Therefore, the problem of equal spacings of HD 24712 can be solved if we assign $l_m = 0$ modes (rather $l_m = 1$ modes) to f1, f3, and f5, and consider that B_p happens to have a value near the crossings between $l_m = 0$ and $l_m = 1$ modes. The solution has some weaknesses, however:

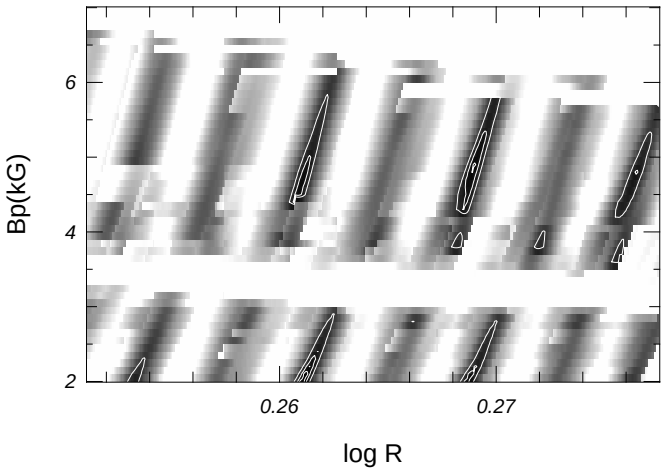

Figure 5. The distribution of the mean deviation of theoretical frequencies from the observed ones on the plane of B_p and stellar radius along the evolution sequence AD165. Darker parts have smaller mean deviations. Contours drawn for mean deviations of 1.5 μHz, 2 μHz, and 3 μHz. The white areas have mean deviations greater than 10 μHz. Although the mean deviation in this diagram was calculated without including $l_m = 0$ modes, the distribution of the mean deviation with $l_m = 0$ modes is similar.

1) For the $l_m = (2, 0, 2)$ combination to become equally spaced, B_p should have a particular value at which the frequency of an $l_m = 0$ mode is just equal to the mean of the two adjacent $l_m = 2$ modes; it looks unlikely for such a coincidence to be realized in α Cir, too; 2) As we will discuss below, the amplitude of an $l_m = 0$ mode modulates with rotation phase differently from the observed total light variations. Nevertheless, we will consider both possibilities for the mode identifications for f1, f3, and f5.

The observed frequencies of HD 24712 were compared to models having $\Delta\nu \sim 68\,\mu$Hz for each evolution sequence listed in Table 1. The quality of the fits was estimated by the mean deviation of model frequencies (for $l_m \leqslant 3$) from the nine observed ones. The WET f7 frequency was not included in calculating the mean deviation because it differs from f6 only by 2.4 μHz and no models can fit both frequencies. In calculating mean deviations, we adopted equal weights for all the frequencies because observational errors are much smaller than the theoretical uncertainties which can be estimated as $\sim 1\,\mu$Hz from the scatter seen in Fig. 4.

Table 2 lists parameters and the mean deviation (MD) of the best-fit model for each model series, where MDs in parentheses refer to the values obtained including $l_m = 0$ modes. Generally, including $l_m = 0$ models yields much better agreement. The positions of these best models on the HR diagram are shown by square symbols in Fig. 2. The position of HD 24712 on the HR diagram is consistent with $1.65\,M_\odot$ model with normal composition and with $1.70\,M_\odot$ model with a heavy-element abundance of $Z = 0.025$. The quality of the frequency fit is practically independent of the type of T–τ relations, helium depletion, or the efficiency of convection. The mean deviations of the best-fit models tend to be smaller when the position of the models on the HR diagram is close to the position spectroscopically determined for HD 24712.

Although Cunha et al. (2003) concluded that a metal-poor abundance was preferred, Table 2 indicates that our metal-poor cases are no better than the other cases. The discrepancy might arise from the fact that their adopted radius of HD 24712, $\log(R/R_\odot) \approx 0.231$, is somewhat smaller than ours.

Table 2. Best fit models

Name	$\log R$	$\log T_{\rm eff}$	$\log L$	B_p	MD(μHz)
AD160	0.2654	3.8471	0.8720	5.3	1.54 (1.09)
AD165	0.2690	3.8585	0.9247	4.9	1.45 (1.04)
AD170	0.2724	3.8696	0.9759	4.6	1.60 (1.05)
AH165	0.2702	3.8581	0.9255	5.5	1.45 (1.03)
AH165C	0.2723	3.8574	0.9267	6.8	1.40 (1.06)
AD170Z25	0.2735	3.8549	0.9192	5.1	1.48 (0.99)
AH170Z25	0.2668	3.8572	0.9150	5.6	1.45 (1.43)
AD150Z1	0.2548	3.8667	0.9291	4.6	1.71 (1.22)
AH150Z1	0.2561	3.8663	0.9299	5.3	1.64 (1.12)
SD160	0.2665	3.8467	0.8726	5.8	1.49 (1.06)
SD165	0.2700	3.8582	0.9253	5.4	1.39 (1.02)
SD170	0.2733	3.8693	0.9764	5.0	1.57 (1.15)
SH165	0.2711	3.8578	0.9260	6.1	1.36 (1.03)

The magnetic field strength for each best fit model is determined mainly by the requirement that the frequency difference between f8 and f6 be equal to the frequency difference $|\nu(n_4+1; l_m=2) - \nu(n_4+1; l_m=3)|$ which varies weakly as a function of B_p (Fig. 3), where n_4 is the radial order for the main frequency f4; i.e., $\nu(n_4; l_m = 2)$ =f4. (We note that at $B_p = 0$, $|\nu(n; \ell = 2) - \nu(n; \ell = 3)|$ is always much larger than the frequency separation between f8 and f6 (or f7).) Since the magnetic field effect on pulsations is stronger in less dense atmospheres for a given frequency and B_p, the required magnetic field strength tends to be smaller for more massive or helium-depleted models. Considering the fact that the spectroscopically determined magnetic field strength is $B_p \approx 4.4$ kG (§ 1), a He-depleted model of AD165 or AD170Z25 is better for the model of HD 24712.

Fig. 5 shows the distribution of the mean deviations on the $\log R - B_p$ plane for AD165 models, where R means stellar radius. Darker parts indicate smaller mean deviations. Theoretical frequencies are interpolated with respect to $\log R$ along the evolutionary model sequence, but not interpolated with respect to B_p (frequencies are obtained at every 0.1 kG).

As stellar radius changes, the oscillation frequencies change with keeping $\Delta\nu$ approximately constant. Therefore, at a fixed B_p the mean deviation becomes small cyclically with varying $\log R$, when regularly spaced observed frequencies (fm1, fm2, and from f1 to f6) become close to $l_m = 1$ and 2 modes. This corresponds to the cyclic appearances of dark bands in Fig. 5.

The dark bands are inclined because oscillation frequencies increase gradually as B_p increases. They are interrupted at $B_p \sim 3.5 - 3$ kG, because oscillation frequencies jump there (see Fig. 3). The darkness of the bands varies alternatively; i.e., the mean deviation is smaller when the frequencies fm2, f2, f4 and f6 are fitted with $l_m = 2$ modes (as at $B_p \approx 4.9$ kG in Fig. 3) rather than with $l_m = 1$ modes, because in the former case the frequency f8 can be fitted well with an $l_m = 3$ mode.

Thus, we identify the main frequency f4 as an $l_m = 2$

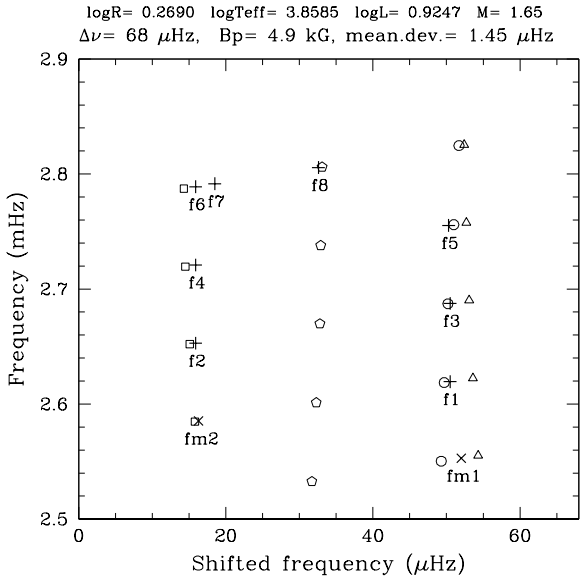

Figure 6. Echelle diagram of frequencies for the best fit model in AD165 and observed frequencies of HD 24712 from the WET campaign (pluses; Kurtz et al. 2005) and from Mkrtichian & Hatzes (2005). Open symbols are model frequencies; circles for $l_m = 0$, triangles for $l_m = 1$, squares for $l_m = 2$ and pentagons for $l_m = 3$.

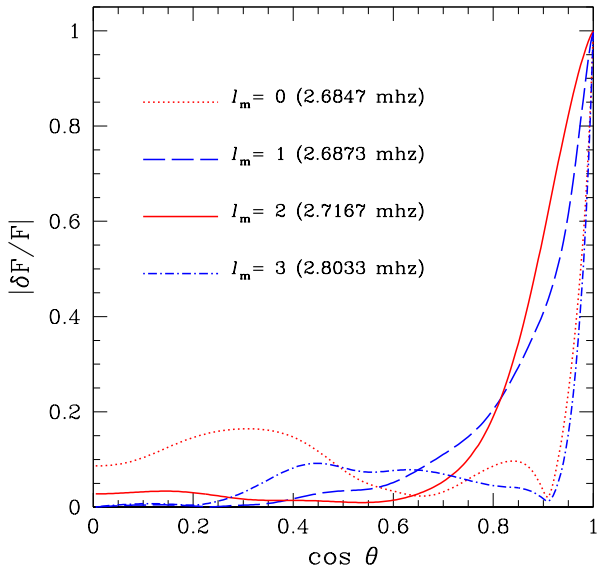

Figure 7. The amplitude of radiative flux variation on the stellar surface as a function of $\cos\theta$ for a model close to the best fit model of AD165, where θ is the co-latitude measured from the magnetic axis. We have chosen one mode for each degree l_m having a frequency close to one of the observed frequencies of HD 24712.

mode because then the highest frequency f8 can be well fitted with an $l_m = 3$ mode. This identification is different from that of Kurtz et al. (2005); they identified f4 as a deformed dipole ($l_m = 1$) mode mainly based on the consistency of the amplitude of rotational side-lobes. We will show below that due to a strong deformation of the amplitude over the stellar surface, the mean amplitude of the rotational side-lobes for f4 agrees with that expected from a $l_m = 2$ mode.

Fig. 6 is an Echelle diagram for the model at $(\log R, B_p) = (0.269, 4.9\mathrm{kG})$ in Fig. 5. It is the best from the family of AD165 models for $B_p > 3\,\mathrm{kG}$ with the mean deviation of the model being $1.45\,\mu$Hz without $l_m = 0$ modes and $1.04\,\mu$Hz if $l_m = 0$ modes are included. (Although a smaller mean deviation of $1.21\,\mu$Hz is realized at $(\log R, B_p) = (0.261, 2.1\mathrm{kG})$, the magnetic field strength in the model is smaller than the observational estimates (§1), and the phase variation in the atmosphere is inconsistent with observation.) Fig. 6 shows that although the large separation of the model agrees very well with observations, the small spacing defined by $l_m = 1$ and $l_m = 2$ modes is too large by about $3\,\mu$Hz. This discrepancy disappears if f1, f3 and f5 are fitted with $l_m = 0$ modes rather than $l_m = 1$ modes. In this case, the nearly equal spacings, $f5 - f4 \approx f4 - f3 \approx f3 - f2 \approx f2 - f1 \approx 34\,\mu$Hz, are realized by pairs of $l_m = 2$ and $l_m = 0$.

In previous investigations the identity of f8 was puzzling because it is separated from f7 (or f6) by only $17\,\mu$Hz, half of the regular spacing. In our models $f8$ can be well fitted with an $l_m = 3$ mode. It is not clear, however, why no other $l_m = 3$ modes are detected.

3.2 Amplitude modulation with rotation phase

Observed pulsation amplitudes of roAp stars change with magnetic (rotation) phase in such a way that the amplitude is maximum at the phase of magnetic maximum. This is interpreted by the oblique pulsator model proposed by Kurtz (1982); i.e., an axisymmetric pulsation mode whose axis aligns with the magnetic axis which is in turn inclined to the rotation axis. As the star rotates one observes pulsations at varying aspect, which causes the amplitude modulation.

HD 24712, like other roAp stars, shows an amplitude modulation with the amplitude maximum occurring at the magnetic maximum as found by Kurtz et al. (1989) (see also Ryabchikova et al. 2007). Theoretically, amplitude modulation of a pulsation mode can be obtained by integrating the amplitude distribution over the stellar disc assuming various values of the angle between pulsation axis (i.e., magnetic axis) and the line-of-sight expected during a rotation period.

Fig. 7 shows the amplitude of radiative flux variation as a function of $\cos\theta$ for individual pulsation modes with various latitudinal degrees l_m for the best model of AD165. θ is the co-latitude with respect to the magnetic axis. The frequency of each mode is close to one of the observed frequencies of HD 24712, though the amplitude distribution is insensitive to the pulsation frequency. Due to the presence of a strong magnetic field, the latitudinal distribution of pulsation amplitude significantly deviates from any single Legendre function $P_\ell(\cos\theta)$. The amplitude around the equatorial region is strongly suppressed and it is more concentrated in the polar regions compared to the non-magnetic case. The $l_m = 0$ case is somewhat different from the other cases; it

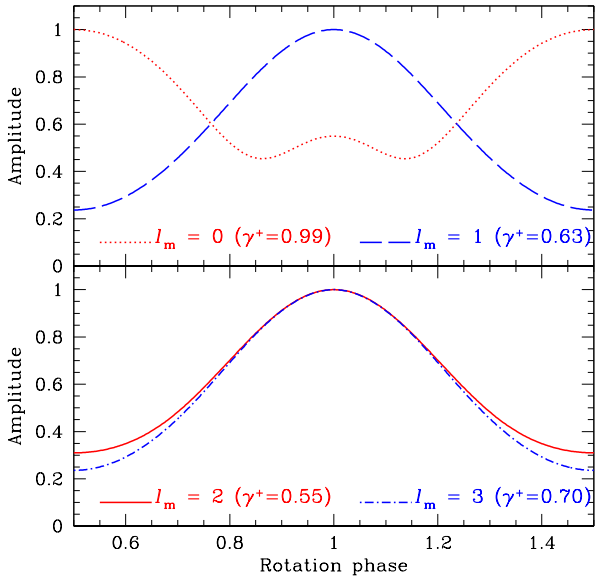

Figure 8. Amplitude modulations with rotation phase in light variations predicted from the amplitude distributions on the stellar surface shown in Fig. 7. We have assumed $i = 137°$ and $\beta = 150°$ according to Bagnulo et al. (1995), and $\mu = 0.6$ for the limb-darkening parameter. The quantity γ^+ is defined as $(A_{-1} + A_{+1})/A_0$ with A_0 and $A_{\pm1}$ being central amplitude and amplitudes of rotational side-lobes, respectively.

has a broad peak around the equator, which significantly influences amplitude modulation as discussed below.

It is remarkable that the amplitude distribution of the $l_m = 1$ mode in the hemisphere is very close to that of the $l_m = 2$ mode except that the latter (former) is symmetric (anti-symmetric) to the equatorial plane. Since we see mostly one magnetic hemisphere of HD 24712, we expect that amplitudes in light variations and rotational amplitude modulations of $l_m = 1$ and $l_m = 2$ modes are comparable to each other.

Fig. 8 shows amplitude modulations predicted from the amplitude distributions shown in Fig. 7, assuming Bagnulo et al.'s (1995) parameters: $i = 137°, \beta = 150°$. Magnetic maximum corresponds to the rotation phase of unity. All the modes except for $l_m = 0$ have maximum amplitudes at magnetic maximum in agreement with the observations by Kurtz et al. (1989).

Despite a considerable difference in the amplitude distributions between $l_m = 1$ and $l_m = 3$ (Fig. 7), the amplitude modulation curves are very similar. This comes from the fact that for an odd mode contributions from components of $\ell \geqslant 3$ to the light variation is very small compared with that of the $\ell = 1$ component, as discussed in Saio & Gautschy (2004).

In contrast to the other cases, amplitude of the $l_m = 0$ mode is maximum at the magnetic minimum, although the modulation amplitude is small. This is caused by a broad peak of amplitude near the equator seen in Fig. 7. The property of the amplitude modulation of the $l_m = 0$ mode indicates that the largest amplitude mode of HD 24712 cannot be matched with a $l_m = 0$ mode, although it is still possible that $l_m = 0$ modes are involved in the pulsations of this star without influencing the total signal very much.

The observed ratio of the minimum to the maximum amplitude can be read as ~ 0.3 from Fig. 1 of Kurtz et al. (1989), which is consistent with the theoretical predictions for $l_m = 1, 2$ and 3. More quantitative comparisons are possible by using rotational side-lobes in the Fourier spectrum. The rotational side-lobes are characterized by the quantity

$$\gamma^+ \equiv \frac{A_{-1} + A_{+1}}{A_0}, \tag{4}$$

where A_0 refers to the amplitude of the central frequency and A_{-1} and A_{+1} refer to the amplitudes of the first lower- and higher-frequency side-lobes, respectively. (For our theoretical side-lobes $A_{-1} = A_{+1}$ because we do not include Coriolis force effects.) The value of γ^+ for each mode in Fig. 8 is indicated in parentheses. The value of γ^+ depends on the latitudinal degree l_m, but it is insensitive to the frequency; i.e., pulsation modes with the same l_m but different radial orders have similar values of γ^+.

Kurtz et al. (2005) obtained γ^+ for each of the frequencies of HD 24712; among them the values for the three main frequencies f2, f3 and f4 are well determined with uncertainties less than 6%. The mean value from 2000 and 1986 data is 0.60 for f4, and 0.64 for f2. We have matched f4 and f2 with $l_m = 2$ modes which have $\gamma^+ = 0.55$ (Fig. 8), not very different from the observed values. On the other hand, the mean value for f3 is 0.83, which is considerably higher than 0.63 expected for an $l_m = 1$ mode. As discussed above and indicated in Fig. 6, f3 is also close to an $l_m = 0$ mode having $\gamma^+ = 0.99$. The observed value of γ^+ lies in the middle between γ^+s of $l_m = 1$ and $l_m = 0$ modes. This could indicate the possibility for the frequency f3 to be a superposition of the $l_m = 1$ and $l_m = 0$ modes.

The amplitudes of the second rotational side-lobes are predicted to be about 10 times smaller than those of the first side-lobes. For example, the amplitude of the second side-lobes of f4 ($l_m = 2$) is expected to be about 30 μmag, which is smaller than the amplitude of the highest noise peaks (80 μmag) in the analysis of Kurtz et al. (2005).

Fig. 9 shows rotational modulations of pulsation phase at $\delta L = 0$ and at $V_{\rm rad} = 0$ (changing from negative to positive) for each mode shown in Fig. 7, where $V_{\rm rad}$ is the radial velocity (RV) at $\log \tau \approx -6$. Except for the $l_m = 0$ case no rapid changes occur in pulsation phase as observed in some other stars (e.g. HR 3831 (HD 83368), Kurtz & Shibahashi 1986; Baldry & Bedding 2000). This is because we see only one magnetic pole of HD 24712 with a configuration of $(\beta, i) = (150°, 137°)$. For the $l_m = 0$ mode rapid changes in pulsation phase occur at the rotation phases ~ 0.8 and ~ 1.2. This comes from the presence of a nodal line at $\cos\theta \approx 0.9$ in the amplitude distribution (Fig. 7).

For the $l_m = 2$ mode (the 2nd panel from the top in Fig. 9), which corresponds to the main frequency f4, the phase of the luminosity variations is nearly constant. The phase of the RV variations is also practically constant in the rotational phase interval $0.75 - 1.25$, although it changes gradually at other phases. Simultaneous spectroscopic and photometric monitoring of HD 24712 (Sachkov et al. 2006) (see also Paper I) performed between rotational phases 0.87 and 1.18 do not show phase variations, thus supporting theoretical predictions. The phase of the luminosity variations is

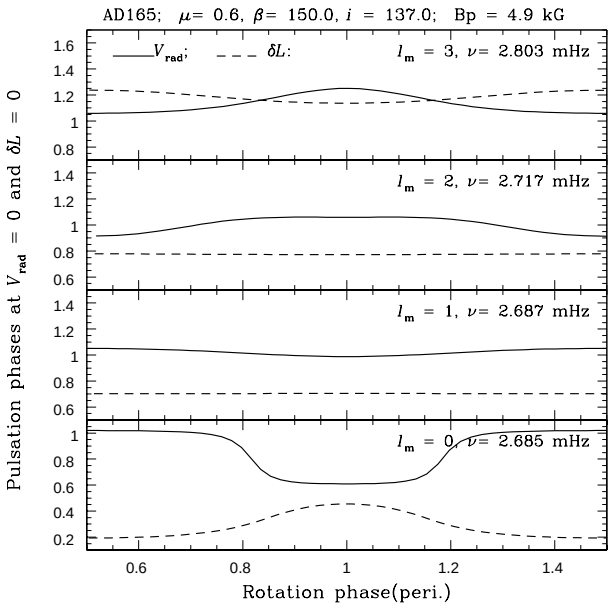

Figure 9. Theoretical oscillation phase modulations in light and velocity variations for each mode shown in Fig. 7. In each panel oscillation phases at $\delta L = 0$ and at $V_{\rm rad} = 0$ (from negative to positive) are plotted as a function of the rotation phase, where $V_{\rm rad}$ refers to the radial velocity at $\log\tau \approx -6$.

Table 3. Phase lags in the outermost layers

Line	λ(Å)	$\log\tau_{5000}$	$\delta\phi$
Pr III	5285	-6.41	0.44
Pr III	5300	-6.35	0.46
Pr III	6160	-6.33	0.42
Pr III	6090	-6.30	0.43
Pr III	6196	-6.29	0.43
Nd III	5294	-6.03	0.33
Nd III	5127	-5.94	0.31
Nd III	4927	-5.79	0.28
Pr III	6707	-5.53	0.37
Pr III	5844	-5.51	0.38
Pr III	5999	-5.50	0.38
Nd III	6145	-5.49	0.28
Pr III	6053	-5.48	0.39
Nd III	5410	-5.44	0.26
Nd III	5988	-5.43	0.27
Nd III	5845	-5.32	0.27

always smaller than that of the RV variations, which means that the maxima (for example) of the luminosity variation precede the maxima of the RV variations. The maximum value of the phase difference is about 0.3 of the period and is realized when the rotation phase is around unity; i.e., when the pulsation amplitude is maximum (Fig. 8). This means that velocity maxima lag luminosity maxima by about 30% of a pulsation period around the rotation phase when oscillation amplitude is maximum.

Ryabchikova et al. (2007) obtained phase lags of RV variations with respect to the light variations for various spectral lines. These phase lags are always negative which means that luminosity maximum occurs after the RV maxima. For two other roAp stars, 10 Aql (Sachkov et al. 2008) and HD 101065 (Mkrtichian et al. 2008), the observed phase lags are positive, in the range $0.4 - 0.6$ (10 Aql) and $0.16 - 0.19$ (HD 101065), respectively. Allowing one cycle for the phase uncertainty, the negative phase lags in HD 24712 may be converted into the positive ones. Table 3 lists some results for the lines formed in the most superficial layers, where optical depth of the formation of each line has been obtained by using a NLTE model of Shulyak et al. (2009). Generally the phase lag $\delta\phi$ decreases with depth, indicating oscillations propagates outward as discussed below. Table 3 shows that the phase lag around $\log\tau \approx -6$ is about $0.3 - 0.4$, roughly consistent with the theoretical prediction for the main frequency.

3.3 Amplitude and phase variations with depth

Ryabchikova et al. (2007) obtained amplitudes and phases of the RV variations in various spectral lines for the two highest amplitude modes (f4 and f2) from time-resolved spectroscopic observations of HD 24712. In the present paper we consider the results at a rotational phase of 0.94 (UVES observations close to the magnetic maximum). For a representative sample of Pr II, Pr III, Nd IIand Nd III lines, as well as for the Hα core, depths of formation were calculated in NLTE approximation (Mashonkina et al. 2005, 2009) using a model atmosphere from Shulyak et al. (2009). In these iterative model calculations empirical stratifications of the chemical elements Si, Ca, Cr, Fe, Sr, Ba, Pr and Nd were derived for each iteration. NLTE calculations were performed for Pr and Nd only, because these elements are concentrated in the uppermost atmospheric layers, while other elements have a tendency to be accumulated close to photosphere where NLTE effects may be neglected. Final element distributions were then used for depth of formation calculations. The results have been converted to the relations between optical depth and RV amplitude/phase. For Y II lines no stratification analysis was performed, therefore, depth of line formation was calculated with a uniform yttrium distribution using an yttrium abundance $\log(Y/N_{\rm tot})$=8.60 derived from abundance analysis.

Figs 10 and 11 compare RV amplitude/phase – $\log\tau_{5000}$ relations for f4 and f2, respectively, with the corresponding theoretical relations of $l_m = 2$ modes for He-depleted best models (Table 2). For Y II and Fe II lines with very low RV amplitudes pulsational phases are plotted twice: as defined originally in Ryabchikova et al. (2007), and shifted downward by a pulsation period taking into account the one-period uncertainty in the phase relation. Similar comparisons for models without He-depletion are given in Figs 12 and 13. In comparing the observed and theoretical relations, the theoretical amplitude is multiplied by an arbitrary factor, and the theoretical phase delay is fitted at the outer boundary ($\log\ \tau \approx -6$) by applying an arbitrary shift.

In the outermost layers oscillation phase gradually delays toward the outer boundary, indicating the presence of running waves propagating outward. This is consistent with the fact that all the observed oscillation frequencies of HD 24712 are larger than the acoustic cut-off frequencies of theoretical models. (If a reflective outer boundary condition is imposed, the phase in the outermost layers is nearly con-

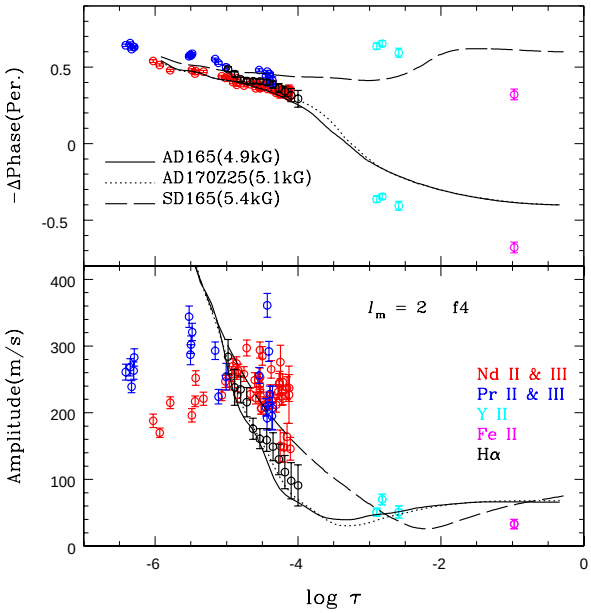

Figure 10. Optical depth versus phase delay (top panel) and amplitude (bottom panel) of RV variations for f4 (the main oscillation mode) obtained from various spectral lines of HD 24712. For Y II and Fe II the phases shifted downward by a pulsation period are also shown. Various lines are theoretical relations for $l_m = 2$ modes having frequencies similar to f4 for some He-depleted models (see Table 1 for parameters of each model). In calculating theoretical relations angles of $(i, \beta) = (137°, 150°)$ are assumed.

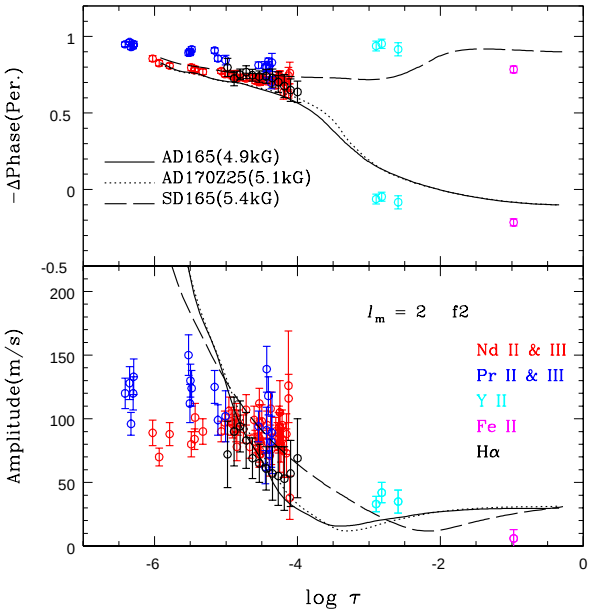

Figure 11. The same as Fig. 10 but for f2.

stant.) The gradient of the phase variation in the outermost layers is well reproduced by theoretical relations. We note that if the dS/dt term in equation (2) is dropped, the gradient becomes steeper, indicating that the Unno & Spiegel (1966) theory is consistent with the observations.

The phase distribution in HD 24712 has a jump between $\tau \approx 10^{-4}$ and 10^{-3} for both f4 and f2, indicating the presence of a quasi-node there. This property agrees with the theoretical phase variations for A-models with the $T - \tau$ relation having a small temperature inversion at $\log \tau \approx -3.5$ (Fig. 1). A rapid phase change in S-models with the standard $T - \tau$ relation, however, occurs between $\tau \approx 10^{-3}$ and 10^{-2}, deeper than the phase jump derived from observations. Thus, the position of the phase jump supports the $T - \tau$ relation with a temperature inversion at $\log \tau \approx -3.5$ as obtained by Shulyak et al. (2009).

Whether the phase of theoretical models jump downward or upward depends on the assumption of helium depletion, and sometimes on the strength of the magnetic field. Generally, phase tends to decrease inward at the quasi-node in helium-depleted models, and to increase inward in models without helium depletion. In the best model of the AH165 series with $B_p = 5.5$ kG, the phase of RV variations for the main frequency f4 decreases steeply inward at $\log \tau \approx -3$, while it *increases* steeply at the same layer if B_p is slightly increased to 5.8 kG (Fig. 12), although for the secondary frequency f2 the phase increases steeply inward for both cases (Fig. 13). However, such a strong dependence of the direction of the phase jump on B_p does not occur in the other cases.

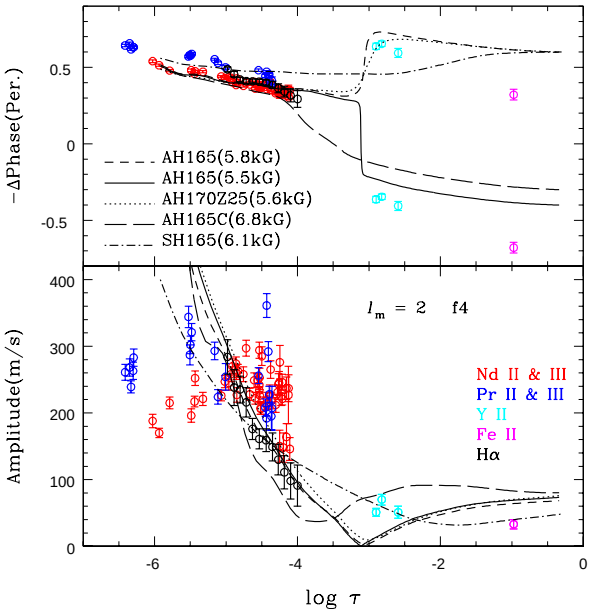

Figure 12. The same as Fig. 10 but compared with models without helium depletion.

To obtain information on the helium depletion in the atmosphere of HD 24712, further observations are needed to fill the gap between $\log \tau = -4$ and -3 .

Towards deep interior, theoretical pulsation phase approaches a constant; i.e., nearly a standing wave is realized in the deep atmosphere. However, the innermost Fe II data for the main pulsation f4 deviate considerably from the theoretical curves. A possible cause may be related to the surface element distribution; Fe is concentrated around the equator,

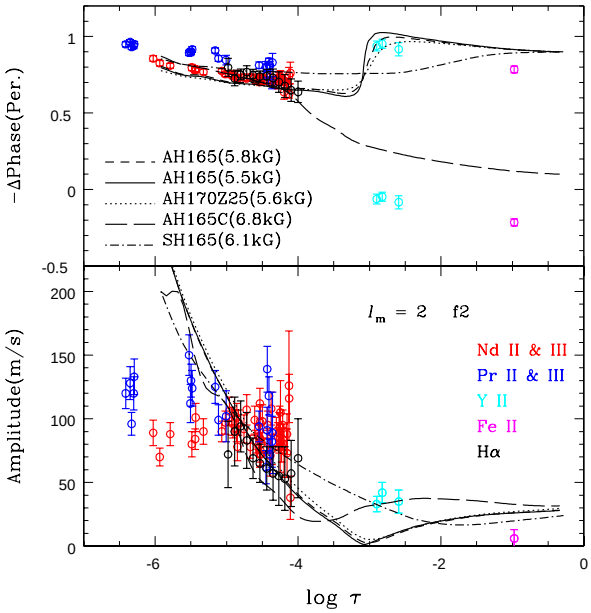

Figure 13. The same as Fig. 12 but for f2.

while Y (as all rare earth elements, including Pr and Nd) is concentrated near magnetic poles (Lüftinger et al. 2008).

Oscillation amplitude increases rapidly in the outermost layers due to a rapid decrease in the gas density. In the layers of $-5 < \log\ \tau < -4$, theoretical amplitude variations roughly agree with the observed ones for both f4 and f2. In the outermost layers with $\log\ \tau < -5$, however, theoretical amplitudes deviate significantly from the observations. Observed amplitudes level off in the most superficial layers, the cause of which is not clear; it could be the effect of nonlinear dissipation, or the density stratification could differ significantly from our simple models.

4 CONCLUSIONS

We discussed theoretical models for the oscillations of the roAp star HD 24712 (HR 1217). Observed frequencies are fitted well with theoretical ones for models whose positions on the HR diagram are close to the position of HD 24712 determined by spectroscopy along with the Hipparcos parallax. The observed main frequency f4 is identified as a quasi-quadrupole ($l_m = 2$) mode, whose amplitude on the surface is strongly concentrated in the polar regions and is suppressed significantly around the equator. The theoretical amplitude distribution predicts a rotational modulation of the pulsation amplitude which is consistent with the observations.

We modelled for the first time the distributions of the phase and amplitude of RV variations as a function of atmospheric height and compared these with the observed distributions. The gradual outward increase of phase lag in the outermost layers is well reproduced by theoretical results obtained with a running-wave outer boundary condition. The presence of a steep phase change between $\log\tau \approx -4$ and -3 favours a $T-\tau$ relation with a temperature inversion at $\log \approx -3.5$, rather than a standard $T-\tau$ relation.

Although our models agree with most of the observed properties of the oscillations in the atmosphere of HD 24712, we have recognized three problems to be solved in the future.

(i) The observed amplitude of velocity variation levels off in the outermost layers with $\log\tau < -5$, while in all the models we have calculated amplitude increases steeply outward in the layers with $\log\tau < -4$.

(ii) If the observed main frequencies are identified with $l_m = 2$ and $l_m = 1$ modes, to explain their nearly equal spacings the small frequency spacing defined as $\nu(n, l_m = 1) - 0.5[\nu(n, l_m = 2) + \nu(n-1, l_m = 2)]$ must be as small as $0.5\,\mu$Hz. For all the models calculated, however, the small spacing was always larger than $\sim 3\,\mu$Hz. The problem goes away if we assume the observed equal spacings of frequencies are produced by $l_m = 2$ and $l_m = 0$ modes rather than $l_m = 2$ and $l_m = 1$ modes. However, this solution has a problem; $l_m = 0$ modes have rotational amplitude modulations different from the modulation seen in the light variations of HD 24712.

(iii) We have found no excited oscillation modes with frequencies appropriate for HD 24712; in other words all the modes examined are damped ones. High-order p-modes in roAp stars are generally thought to be excited by the κ-mechanism in the hydrogen ionization zone (Balmforth et al. 2001; Cunha 2002). However, the κ-mechanism does not seem to be strong enough to excite the super-critical high-order p-modes in HD 24712. It is interesting to note that the inefficiency of the κ-mechanism is in common with the case of another cool roAp star HD 101065 having many regularly spaced frequencies (Mkrtichian et al. 2008). Probably we need to find a new excitation mechanism for these coolest roAp stars.

ACKNOWLEDGMENTS

We thank Dr. L. Mashonkina for providing us with the numerical data on the NLTE Pr-Nd line depth formation. HS thanks Chris Cameron for stimulating discussions. This work was supported by research grants from the RFBI (08-02-00469a and 09-02-00002a) and from Leading Scientific School (4354.2008.2) to TR and MS.

REFERENCES

Bagnulo S., Landi Degl'Innocenti E., Landolfi M., Leroy J. L., 1995, A&A, 295, 459
Baldry I. K., Bedding T. R., 2000, MNRAS, 318, 341
Balmforth N. J., Cunha M. S., Dolez N., Gough D. O., Vauclair S., 2001, MNRAS, 323, 362
Bigot L., Dziembowski W.A., 2002, A&A, 391, 235
Bigot L., Provost J., Berthomieu G., Dziembowski W. A., Goode P. R., 2000, A&A, 356, 218
Bruntt H., Kurtz D. W., Cunha M. S., Brandão I. M., Handler G., Bedding T. R., Medupe T., Buzasi D. L., Mashigo D., Zhang I., van Wyk F., 2009, MNRAS, 396, 1189
Cunha M. S. 2002, MNRAS, 333, 47
Cunha M. S. 2006, MNRAS, 365, 153

Cunha M. S., Fernandes J. M. M. B., Monteiro M. J. P. F. G., 2003, MNRAS, 343, 831
Cunha M. S., Gough D. O., 2000, MNRAS, 319, 1020
Dziembowski W. A., Goode P. R., 1996, ApJ, 458, 338
Gautschy A., Saio H., Harzenmoser H., 1998, MNRAS, 301, 31
Gruberbauer M., Saio H., Huber D., Kallinger T., Weiss W. W., Guenther D. B., Kuschnig R., Matthews J. M., Moffat A. F. J., Rucinski S., Sasselov D., Walker G. A. H., 2008, A&A, 480, 223
Huber D., Saio H., Gruberbauer M., Weiss W. W., Rowe J. F., Hareter, M., Kallinger T., Reegen P., Matthews J. M., Kuschnig R., Guenther D. B., Moffat A. F. J., Rucinski S., Sasselov D., Walker G. A. H., 2008, A&A, 483, 239
Iglesias C. A., Rogers R. J., 1996, ApJ, 464, 943
Kurtz D. W., 1981, IBVS, 1915, 1
Kurtz D. W., 1982, MNRAS, 200, 807
Kurtz D. W., Cameron C., Cunha M. S., Dolez N., Vauclair G., Pallier E., Ulla A., Kepler S. O., da Costa A., Kanaan A. *et al.*, 2005, MNRAS, 358, 651
Kurtz D. W., Matthews J. M., Martinez P., Seeman J., Cropper M., Clemens J. C., Kreidl T. J., Sterken C., Schneider H., Weiss W. W., Kawaler S. D., Kepler S. O., 1989, MNRAS, 240, 881
Kurtz D. W., Shibahashi H. 1986, MNRAS, 223, 557
Lüftinger T., Kochukhov O., Ryabchikova T., Piskunov N., Weiss W. W., Ilyin I., 2008, CoSka, 38, 335
Mashonkina L., Ryabchikova T., & Ryabtsev A., 2005, A&A, 441, 309
Mashonkina, L., Ryabchikova, T., Ryabtsev, A., Kildiyarova, R., 2009, A&A, 495, 297
Matthews J.M., Kurtz D.W., Martinez P., 1999, ApJ, 511, 422
Matthews J. M., Wehlau W. H., Walker, G. A. H., Yang S., 1988, ApJ, 324, 1099
Mkrtichian D. E., Hatzes A. P., 2005, A&A, 430, 263
Mkrtichian D. E., Hatzes A. P., Saio H., Shobbrook R. R., 2008, A&A, 490, 1109
Ryabchikova T., Landstreet J. D., Gelbmann M. J., Bolgova G. T., Tsymbal V. V., Weiss W. W., 1997, A&A, 327, 1137
Ryabchikova T., Sachkov M., Weiss W. W., Kallinger T., Kochukhov O., Bagnulo S, Ilyn I., Landstreet J. D., Leone F., Lo Curto, G., Lüftinger T., Lyashko D., Magazzù A., 2007, A&A, 462, 1103 (Paper I)
Sachkov, M., Ryabchikova, T., Bagnulo, S., et al., 2006, CoAst, 147, 97
Sachkov, M., Kochukhov, O., Ryabchikova, T., Huber, D., Leone, F., Bagnulo, S., Weiss, W. W., 2008, MNRAS, 389, 903
Saio H., 2005, MNRAS, 360, 1022
Saio H., 2008, JPhCS, 118, 012018
Saio H., Cox J.P., 1980, ApJ 236, 549
Saio H., Gautschy A., 2004, MNRAS, 350, 485
Shibahashi H., Saio H., 1985, PASJ, 37, 245
Shulyak D., Ryabchikova T., Mashonkina L., Kochukhov O., 2009, A&A, 499, 879
van Leeuwen F., 2007, Hipparcos, the New Reduction of the Raw Data, Astrophysics and Space Science Library, Springer
Wade G. A., 1997, A&A, 325, 1063
Unno W., Osaki Y., Ando H., Saio H., Shibahashi H., 1989, Nonradial Oscillations of Stars. Univ. of Tokyo Press, Tokyo
Unno W., Spiegel E. A., 1966, PASJ, 18, 85